

III - A15 A Unified Elastoplastic Model for Clay and Sand with the SMP Criterion

Nagoya Institute of Technology MJSCE ○ Hajime Matsuoka
Nagoya Institute of Technology Yang-Ping Yao
Nagoya Institute of Technology MJSCE De'An Sun

1.Introduction: In the modified Cam-clay model, the criterion of the Extended Mises type was adopted for the shear yield and failure of clay. The plastic volumetric strain ϵ_v^p is taken as its hardening parameter. However, it is well known that the failure of soil is not explained by the criterion of the Extended Mises type but by the criterion of the Mohr-Coulomb type or the SMP type (Matsuoka and Nakai, 1974) and others. The hardening parameter ϵ_v^p is also not appropriate for sand. Taking the consistency in the shear deformation and the shear failure into consideration, it is quite natural to introduce the criterion of the SMP type for the shear yield as well as the shear failure of soil. In this paper, the method for the transformation of the curved surface of the SMP criterion to a cone in the transformed principal stress space is proposed by introducing a transformed stress $\tilde{\sigma}_i$. The

transformed stress $\tilde{\sigma}_i$ is applied to the modified Cam-clay model. The revised modified Cam-clay model has realized the consistency from the shear yield to the shear failure of clay and the combination of the idea of critical state theory with the SMP criterion. Figure 1 shows the shapes of the SMP criterion in the ordinary principal stress space (Fig.1(a)) and the transformed principal stress space (Fig.1(b)), respectively. On the other hand, taking the consistency of the constitutive model for clay and sand, a new hardening parameter H is proposed, which can not only describe the dilatancy of sand, but also be reduced to ϵ_v^p for normally consolidated clay.

2. A New Transformed Stress Tensor Based on SMP Criterion: One of the failure criteria to explain well the recent test results of soil is the SMP failure criterion which can be written as

$$\frac{\tau_{SMP}}{\sigma_{SMP}} = \sqrt{\frac{I_1 I_2 - 9I_3}{9I_3}} = \text{const.} \quad \text{or} \quad \frac{I_1 I_2}{I_3} = \text{const.} \quad (1)$$

where τ_{SMP} and σ_{SMP} are the shear and normal stresses on the SMP. When the value of $\tau_{SMP} / \sigma_{SMP}$ is given, the shape and size of the SMP criterion in the principal stress space (Fig.1(a)) is determined. The length of OC ($=\ell_0$) shown in Fig.2(a) for a given p can be expressed in the following function.

$$\begin{aligned} \ell_0 &= \sqrt{\frac{2}{3}} q_c = \frac{2\sqrt{6}p}{3\sqrt{1+8(\tau_{SMP}/\sigma_{SMP})^2/9-1}} \\ &= \sqrt{\frac{2}{3}} \frac{2I_1}{3\sqrt{(I_1 I_2 - I_3)/(I_1 I_2 - 9I_3)} - 1} \end{aligned} \quad (2)$$

In order to transform the curve of the SMP criterion in the π -plane of σ_i space (Fig.2(a)) into a circle in the π -plane of $\tilde{\sigma}_i$ space (Fig.2(b)) under the same angle ($\theta = \tilde{\theta}$) and the same mean value ($p = \tilde{p}$), the following equations can be made:

$$\tilde{\theta} = \theta, \quad \tilde{p} = p \quad \text{and} \quad \tilde{\ell} = \ell_0 \quad (3)$$

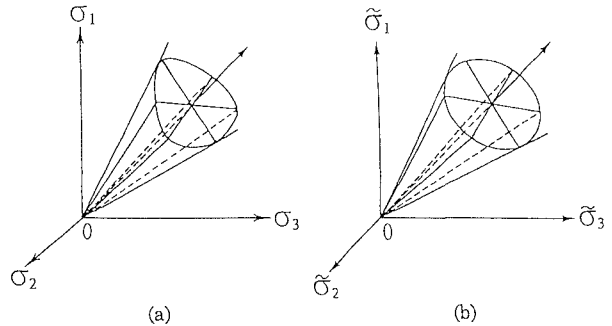


Fig.1. Shapes of SMP failure criterion expressed in (a) ordinary principal stress space and (b) transformed principal stress space

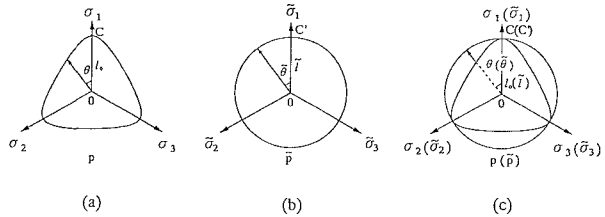


Fig.2. Transformation from SMP curve to circle in π -plane (a) SMP criterion in ordinary stress space, (b) SMP criterion in transformed stress space, and (c) transformation method

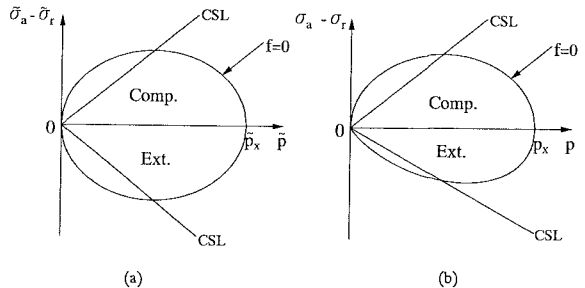


Fig.3. Yield curves of proposed model under triaxial compression and triaxial extension conditions expressed in (a) transformed stress plane and (b) ordinary stress plane

Key words: Constitutive model, Clay, Sand, Dilatancy

Corresponding address: Gokiso-cho, Showa-ku, Nagoya, 〒466-8555, TEL.052-735-5483, FAX 052-735-5483, 5503

where θ and $\bar{\theta}$ are Lode's stress angles (Fig.2(c)). The transformed stress tensor $\bar{\sigma}_{ij}$ can be obtained by solving Eq.(3) as follows ($\bar{q} = q_c$):

$$\bar{\sigma}_{ij} = p \delta_{ij} + \frac{q_c}{q} (\sigma_{ij} - p \delta_{ij}) \quad \text{or} \quad \frac{\bar{\sigma}_{ij} - \bar{p} \delta_{ij}}{\bar{q}} = \frac{\sigma_{ij} - p \delta_{ij}}{q} \quad (4)$$

When the stress tensor σ_{ij} is given, the transformed stress tensor $\bar{\sigma}_{ij}$ can be calculated from Eqs.(2) and (4).

3. A Unified Elastoplastic Model for Clay and Sand with the SMP Criterion: The plastic potential function / yield function is written as the modified Cam-clay model's:

$$f = g = \frac{\lambda - \kappa}{1 + e_0} \ln \frac{\bar{p}}{\bar{p}_0} + \frac{\lambda - \kappa}{1 + e_0} \ln \left(1 + \frac{\bar{q}^2}{M^2 \bar{p}^2} \right) - H = 0 \quad (5)$$

Here, H is a new hardening parameter, which increases monotonously as loading, and can be assumed as

$$H = \int dH = \int \frac{M^4}{M_u^4} \frac{M_u^4 - \bar{\eta}^4}{M^4 - \bar{\eta}^4} d\epsilon_v^p \quad (6)$$

where, $\bar{\eta}$ is stress ratio \bar{q}/\bar{p} , M phase transformation stress ratio, M_u ultimate stress ratio which is a little larger than M_f (stress ratio at failure), $d\epsilon_v^p$ plastic volumetric strain increment. For normally consolidated clay, $H = \epsilon_v^p$ because $M = M_u$. This realizes a unified elastoplastic model for sand and clay.

From Eq.(6), we can get

$$d\epsilon_v^p = \frac{M_u^4}{M^4} \frac{M^4 - \bar{\eta}^4}{M_u^4 - \bar{\eta}^4} dH \quad (7)$$

Because dH is always larger than or equal to 0, the following conclusions can be obtained:

- (1) $\bar{\eta} = 0$, isotropic consolidation condition, $d\epsilon_v^p = dH$;
- (2) $0 \leq \bar{\eta} < M$, negative dilatancy condition, $d\epsilon_v^p > 0$;
- (3) $\bar{\eta} = M$, phase transformation condition, $d\epsilon_v^p = 0$;
- (4) $M < \bar{\eta} \leq M_f$, positive dilatancy condition, $d\epsilon_v^p < 0$;
- (5) $\bar{\eta} = M_f$, shear failure condition,

$$d\epsilon_v^p = M_u^4 (M^4 - M_f^4) / [M^4 (M_u^4 - M_f^4)] dH.$$

From Eqs.(5) and (6), the following equation can be obtained by the consistency condition:

$$\Lambda = \frac{M_u^4}{M^4} \frac{M^4 - \bar{\eta}^4}{M_u^4 - \bar{\eta}^4} \left(\frac{\partial f}{\partial \bar{p}} d\bar{p} + \frac{\partial f}{\partial \bar{q}} d\bar{q} \right) / \frac{\partial f}{\partial \bar{p}} \quad (8)$$

Figure 3 shows the yield curves of the proposed model in the transformed and ordinary meridional planes, respectively. It is seen from Fig.3 that although the yield curves under triaxial compression and triaxial extension are symmetrical about \bar{p} axis in the $\bar{p} \sim (\bar{\sigma}_s - \bar{\sigma}_t)$ plane (Fig.3(a)), the yield curves are not symmetrical with respect to p axis, and the value of q in triaxial extension is less than that in triaxial compression in the $p \sim (\sigma_s - \sigma_t)$ plane at the same p (Fig.3(b)).

4. Prediction vs. Experiment: The capability of the proposed model in predicting drained behavior of normally consolidated Fujinomori clay and saturated Toyoura sand (experimental data from Nakai and Matsuoka 1983) under triaxial compression and extension conditions has been examined (Fig.4). The values of soil parameters used in the model are $M=M_u=1.36$, $\lambda/(1+e_0)=0.0508$, $\kappa/(1+e_0)=0.0112$, $\nu=0.3$ for Fujinomori clay, and $M=0.95$, $M_u=1.66$, $\lambda/(1+e_0)=0.00403$, $\kappa/(1+e_0)=0.00251$, $\nu=0.3$ for Toyoura sand. It can be seen from Fig.4 that the results (solid lines) predicted by the proposed model agree well with the test results (mark \bigcirc) in triaxial compression and extension conditions. Therefore, in the proposed model, the consistency from triaxial compression to the other three-dimensional stress condition, and from sand to clay, has been realized by introducing a transformed stress $\bar{\sigma}_{ij}$ and a hardening parameter H .

References:

- 1) Matsuoka, H., Yao, Y. P. and Sun, D. A.(1998): "A Transformed Stress Based on SMP Criterion and Its Application to Cam-clay models", Proc. of the 33th Japan National Conference on Geotechnical Engineering (in print).
- 2) Nakai, T. and Matsuoka, H.(1983): "Shear Behaviors of Sand and Clay under Three-dimensional Stress Condition", Soils and Foundations, Vol.23, No.2, pp.26-42

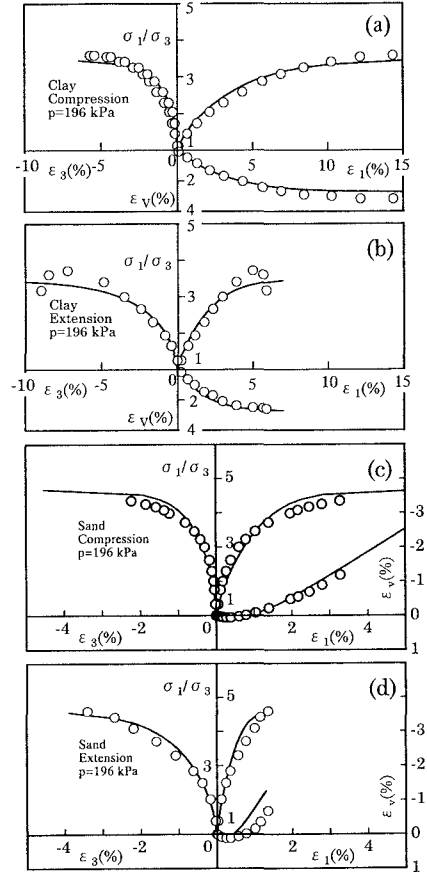


Fig.4. Comparison between predicted and experimental results under triaxial stress conditions (Data after [2])